DNA cut-ligation cyclization surpasses J-Factor limit by more than threefold

Roman Teo Oliynyk[1*] and George M. Church[1,2]

[1*]Department of Genetics, Harvard Medical School, Boston, MA, USA.

[2]Wyss Institute for Biologically Inspired Engineering at Harvard University, Boston, MA, USA.

*Corresponding author(s). E-mail(s): roli573@aucklanduni.ac.nz;

Abstract

We demonstrate DNA circularization efficiencies more than threefold greater than those predicted by classical Jacobson–Stockmayer theory – a cornerstone physical model unchallenged for over seven decades – even at high DNA concentrations suitable for routine practical use. This breakthrough performance is enabled by simultaneous restriction cutting and ligation of double-stranded DNA fragments using the Type IIS enzyme BsaI-HFv2 in combination with T4 DNA ligase under finely optimized buffer conditions. These results unveil a biologically derived exception that overcomes the longstanding physical barriers to DNA cyclization imposed by Jacobson–Stockmayer theory, while highlighting the potential for systematic exploration of enzyme combinations to identify additional systems achieving comparable or superior intramolecular ligation efficiency.

Introduction

Starting with the seminal 1950 Jacobson–Stockmayer theory of the J-factor [1], dozens of studies have addressed DNA circularization and polymerization kinetics [2–7]. The basic principle states that, at sufficient DNA length and concentration, long linear chains predominate, whereas low concentration and short length favor circular species. A notable exception has been reported in

polymer chemistry, for example "Synthesis of cyclic polymers and flaws of the Jacobson–Stockmayer theory" [8].

Calculations based on the J-factor predict far lower circularization efficiencies than the high yields we originally reported using a simultaneous cut-and-ligation method [9]. There we found that the specific combination of the Type IIS restriction enzyme BsaI-HFv2 with T4 DNA ligase in a simultaneous cut-and-ligation reaction yields exceptionally high circularization efficiency that exceeds classical predictions by more than threefold. The exact mechanism remains unknown; we hypothesize that it arises from a mechanism akin to the synapsis of two recognition sites in cis commonly observed in many Type IIS restriction enzymes [10], leading to transient intra-segment colocalization (processive in cis) of the two DNA ends. This colocalization likely assists ligation by T4 DNA ligase, which otherwise depends on the much lower probability of random encounters between the ends via diffusional collision. We have not observed this dramatic enhancement with every common Type IIS enzyme producing 4-nucleotide overhangs (BbsI underperformed pre-cut overhangs, while Esp3I produced substantial but lesser improvement; see Supplementary Note 2) or with pre-cut dsDNA overhangs [11]; however, the discovery of other systems that perform as well or better remains possible.

In this study, we present a further optimized simultaneous cut-and-ligation method that improves upon prior performance within the previously reported practical length range (452–952 bp). A comprehensive review of the DNA circularization literature is provided in our earlier publications [9, 11], upon which the present work builds. These refinements yield circularization efficiencies 3.4 times higher than the long-assumed theoretical limits of the Jacobson–Stockmayer model (equivalently, the cyclization efficiency measured using pre-cut and purified dsDNA overhangs), even at high DNA concentrations suitable for practical applications.

These results demonstrate that the enzyme pair BsaI-HFv2 + T4 DNA ligase, under optimized buffer conditions, constitutes a biologically derived exception that overcomes the classical Jacobson–Stockmayer limitations as well as subsequent theoretical and simulation-based models that have reinforced the same fundamental physical constraints on DNA cyclization efficiency.

Results

The principle and steps of the simultaneous cut-ligation method are schematically presented in Figure 1; for specifics refer to the figure legend and the full protocol [11]. Experiments used the identical dsDNA sequences as in the original report [9] across the 452–952 bp range with 12-hour circularization. This study demonstrates that the combination of NEB BsaI-HFv2 and T4 DNA ligase in a one-pot reaction routinely exceeds Jacobson–Stockmayer predictions by more than threefold at high DNA concentrations that make the method practically useful. To validate higher circularization efficiency at lower DNA concentrations, in addition to the standard concentration of 120 ng/μl, we also

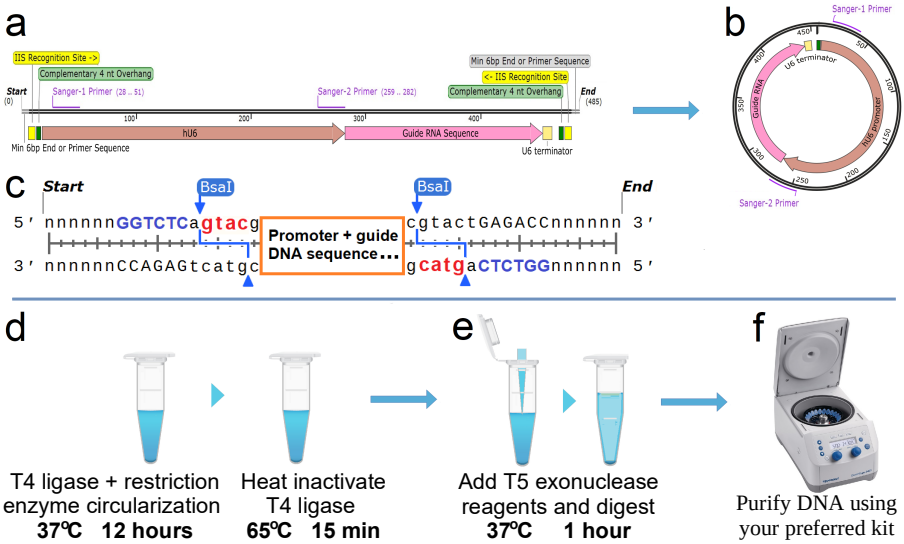

Fig. 1 Simultaneous cut-ligation method and circularization steps. (**a**) dsDNA containing type IIS restriction enzyme recognition sites with complementary overhangs on both ends of the DNA fragment. (**b**) Cuts by the restriction enzyme and ligation of the resulting overhangs form the circular DNA expression element. (**c**) Schematic view of complementary 4nt overhangs.
Method steps: (**d**) Circularization. (**e**) T5 exonuclease digestion of non-circular DNA in one-pot reaction. (**f**) Spin column cleanup. (adapted from Oliynyk & Church (2022)[9])

performed experiments at 60 ng/μl and 30 ng/μl – expected to exhibit higher circularization efficiency. We followed the published conditions, with slight but important modifications in reagent formulations in the T5 exonuclease digestion step that further improved recovery of circular products compared to previously published yields [9] for the smallest minicircle sizes of 452 and 552 bp (see Methods for details).

The modified digestion buffer efficiently eliminates linear DNA, as seen in the ligation/digestion test for all DNA lengths and three DNA concentration scenarios (30, 60 and 120 ng/μl). For this test, we performed the ligation using reagents listed in Methods Table 2 followed by heat inactivation (Figure 1d), shown as digestion time 0 min – no digestion – on the plots Figure 2a–d. Then, we proceeded to the digestion step (Figure 1e), adding T5 Exonuclease and associated reagents as per Methods Table 3, and taking samples for gel imaging at 30 min intervals, each sample spin-column purified (Figure 1f) before gel imaging. The 0 min digestion lanes in Figure 2a–d show that at 452 bp the circularization is most effective, resulting in the smallest amount of linear concatemers compared to the larger minicircles. There is only the faintest trace of linear product for 452 bp minicircles after the ligation step – lane 0 min in Figure 2a at DNA concentration of 30 ng/μl – indicating almost 100% circularization efficiency; at 60 ng/μl the linear product in lane 0 min becomes more prominent, and even more so at 120 ng/μl. The same observation applies

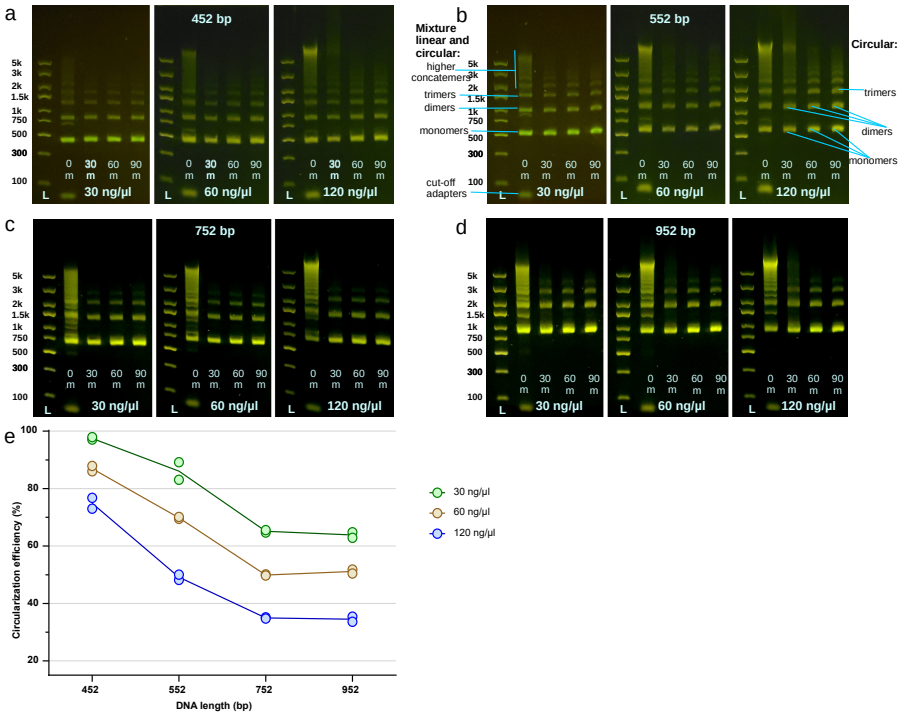

Fig. 2 DNA band distribution following circularization and validation of T5 exonuclease digestion. (**a**–**d**) Agarose gels showing the time-course of T5 exonuclease digestion for the four minicircle lengths (452, 552, 752, 952 bp) each containing subplots at 30, 60 and 120 ng/μl concentrations of source dsDNA (unmodified gel photos are available in Supplementary Data). "L" = gel ladders. "0 min" lanes = product immediately after circularization step (heat-inactivated, no T5 added yet). Subsequent lanes = 30 min, 60 min and 90 min of T5 digestion (each sample purified on spin column before loading). See Supplementary Figures 2–7 for unmodified gel images. (**e**) DNA circularization efficiency (corrected for column recovery losses; n=2 duplicate reactions, individual values shown).

to the circularization efficiency of longer minicircles; however, the amount of linear concatemers in the 0 min bands increases with minicircle size even for the lowest input DNA concentration (Figure 2b–d). There is almost complete disappearance of the high-molecular-weight linear concatemers after 30 min digestion, with remaining non-circular DNA digested by 60 min, and the band pattern remaining unchanged for 90 min digestion samples, indicating that 60 minutes of T5 exonuclease digestion is sufficient for the purposes of our method.

The simultaneous cut-ligation method was performed in duplicate for all 4 DNA lengths and three concentrations, with the results reported in Figure 2e and Table 1. Our validation experiments of the QIAquick spin-column using 452 bp minicircle product as input showed DNA recovery after one cycle of cleanup equal to 0.88, which we rounded to 0.9. Here we are primarily interested in pure circularization efficiency, thus the yields are adjusted by this value to compensate for the cleanup losses (essentially, dividing the measured yield of

DNA by 0.9). Higher circularization efficiency is observed near the optimum J-factor for DNA sizes of ∼452 bp (see also explanation in Methods); thus, at DNA concentration 30 ng/μl circularization efficiency is the highest (97.5%) at 452 bp and lower for each longer DNA length (see Table 1). The circularization efficiency is lower at 60 ng/μl, and lower yet at 120 ng/μl, still remaining impressively high for all four DNA sizes (seen in Figure 2e and Table 1). The lower the circularization efficiency reported in Figure 2e and Table 1, the higher the visible amount of high-order concatemers seen in the corresponding 0 min lanes (post-circularization but pre-digestion) in Figure 2a–d.

We empirically determined the circularization efficiency using pre-cut and purified dsDNA overhangs designed to produce identical circular vector, and the J-factor corresponding to such circularization rate (see Supplementary Note 1, Supplementary Figures 1,8,9 and Supplementary Table 1). The striking difference from standard modeling, which is equivalent to using pre-cut and purified dsDNA overhangs, is a 3.4-fold higher circularization efficiency than would be expected, as can be seen in Table 1, comparing the experimental efficiency (first row in each concentration section) and the expected theoretical performance (second row in each concentration section). With this method, the combination of BsaI-HFv2 and T4 DNA ligase, when used in simultaneous cut-and-ligation with optimal buffer components, exceeds the physics model circularization efficiency by 3.4-fold (75% vs 21.9% yield at the highest DNA concentration).

Table 1 Experimental circularization efficiency of the optimized simultaneous cut-ligation method versus classical Jacobson–Stockmayer physics predictions. The BsaI-HFv2 + T4 DNA ligase combination exceeds theoretical expectations 3.4-fold at high input DNA concentrations for the shortest minicircles.

		Circularization efficiency per minicircle size			
Input DNA	**Data source**	**452 bp**	**552 bp**	**752 bp**	**952 bp**
30 ng/μl	Method	97.5%	86%	65%	64%
	Physics model	59.8%	55.7%	49.9%	45.6%
60 ng/μl	Method	87%	70%	50%	51%
	Physics model	38.1%	34.8%	30.7%	27.1%
120 ng/μl	Method	**75%**	49%	35%	34%
	Physics model	**21.9%**	19.7%	16.8%	14.9%

The spreadsheet for experimental reaction yields and calculations of circularization efficiency is available in the Supplementary Data. The theoretical model estimates are provided in Methods Table 7

In marked contrast to the above results, as has been known for many decades, the same conditions with other common Type IIS enzymes (exemplified by BbsI; see Supplementary Figures 1,10,11 and Supplementary Table 1) yield low circularization efficiencies. In the case of BbsI, it under-performed the values expected based on the empirically known J-factor, yielding only 12.8% minicircle DNA in the same scenario – approximately 42% lower than the J-factor prediction of 21.9% and more than fivefold lower than with

BsaI-HFv2. Revealing that simultaneous cut-ligation with other enzymes may also result in lower than pre-cut DNA circular yield, opposite to the higher yield demonstrated by BsaI-HFv2. Esp3I also produced circularization efficiencies substantially higher than those expected from the J-factor (2.3-fold higher than pre-cut overhangs at 120 ng/μl but lower than Bsai-HFv2; see Supplementary Note 2, Supplementary Figures 1,12).

It is worth noting that, even though lower DNA concentrations with constant enzyme concentration show exceptional efficiency, PCR amplification of dsDNA is inexpensive, requires smaller quantities of reagents, and involves smaller reaction volumes that are easier to handle than the high volumes required at lower DNA concentrations; thus, we consider the 120 ng/μl DNA concentration more cost-effective for practical use.

At the practical level, achieving high circularization at 120 ng/μl for the shortest minicircles makes this method by far the most efficient currently available for producing small circular DNA vectors, with common applications in gRNA expression for CRISPR-Cas genome editing [9, 11].

Discussion

The primary message of this study is: after more than 70 years of DNA cyclization being considered physically constrained by the Jacobson–Stockmayer J-factor, we show that the specific combination of BsaI-HFv2 and T4 DNA ligase in a simultaneous cut–ligation reaction with optimized buffer conditions overcomes these presumed fundamental limitations, delivering circularization efficiencies more than threefold higher than predicted by classical theory.

This exceptional performance has been observed only with the BsaI-HFv2 and T4 DNA ligase combination among the systems tested; no other Type IIS enzyme or pre-cut overhang system we examined shows comparable efficiency. Interestingly, Esp3I also produced circularization efficiencies substantially higher than those expected from the J-factor (2.3-fold higher than pre-cut overhangs at 120 ng/μl; see Supplementary Note 2), although still clearly inferior to BsaI-HFv2.

This result shows that the circularization outcome may depend on the dynamics of restriction enzyme binding and cutting of two recognition sites on one DNA molecule. We theorized based on published research [10] that circularization efficiency improves when a restriction enzyme like BsaI or Esp3I cuts both recognition sites before releasing the DNA, thus leading to transient intra-segment colocalization (processive in cis) of the two DNA ends assisting ligation by T4 DNA ligase. Esp3I, while not as efficient as BsaI, significantly exceeded the ligation efficiency of pre-cut overhangs.

The results exhibited by BbsI lead to a hypothesis that this enzyme cuts only one restriction site at a time, without intra-segment colocalization, and perhaps even shields the second cut location for some time, interfering with cis ligation. The earlier cut DNA end is meanwhile free for trans ligation and diminished circularization efficiency.

The phenomenon therefore represents a biologically derived exception – and possibly a family of such exceptions – to a long-standing physical model that has shaped understanding of DNA cyclization since the 1950s.

In summary, these findings demonstrate that the classical Jacobson–Stockmayer theory, while remarkably robust for seven decades, does not represent an absolute physical barrier when specific enzyme systems are employed for DNA circularization. By showing that very high circularization efficiencies are achievable in practice, this work removes a long-standing conceptual constraint and should encourage the broader community to pursue systematic screening of restriction enzymes, ligases, and accessory factors to discover additional high-performance systems and to elucidate their molecular mechanisms.

Methods

Experimental: Fine-tuning the digestion of linear DNA

The previously published methods [9, 11] were designed to provide a robust, reliable, and user-friendly approach for producing circular DNA vectors, prioritizing simplicity and consistency for routine laboratory applications.

In the present study, our primary objective was to explore and demonstrate the maximum achievable circularization efficiency under optimized conditions. To this end, we introduced targeted refinements to the reaction buffers, aimed at minimizing potential over-digestion by T5 exonuclease – particularly for the smallest, highly curved minicircles that may exhibit transient structural breathing due to A/T-rich regions and potential hairpin-forming sequences in the hU6 promoter [12]. These modifications include reversion to the NEB T4 DNA ligase buffer (pH 7.5) for the circularization step and supplementation of the digestion buffer with 60 mM potassium acetate (KOAc) to enhance DNA stability, reduce breathing, and moderately attenuate T5 exonuclease activity while preserving efficient removal of linear DNA.

The modified buffer compositions are summarized below (Tables 2 and 3). For comprehensive step-by-step instructions, including thermocycling parameters, reagent preparation, and general procedures, readers are referred to the original published method [9, 11].

Through experimental fine-tuning of the digestion buffer components and T5 exonuclease concentrations, we achieved complete digestion of all non-circular DNA. Digestion time-course gels revealed traces of high-molecular-weight concatemers remaining in some samples after 30 min, with complete removal of linear species by 60 min and no further changes in band patterns after 90 min (Figure 2a–d), confirming that 60 min is sufficient for exhaustive digestion of non-circular DNA.

Here we provide a summary of the ingredients that were modified for better performance; refer to [11] for detailed instructions. Sufficient dsDNA was prepared by PCR as described in our 2025 method [11] and DNA concentration adjusted to 300 ng/μl. This DNA was combined into the circularization buffer

Table 2 Circularization reaction ingredients

Component	100 μl reaction	Final conc.
dsDNA - 300 ng/μl	10, 20, 40 μl	30, 60, 120 ng/μl
10X T4 DNA Ligase Buffer (10X B0202S)	10 μl	1X
T4 DNA Ligase (NEB M0202L, 400 units/μl)	6 μl	24 units/μl
BsaI-HFv2 (NEB R3733L, 20 units/μl)	6 μl	1.2 units/μl
ATP (NEB P0756S, 10 mM)	10 μl	1 mM
Nuclease-free H_2O (Invitrogen 10977015)	up to 100 μl	n/a

in Table 2 in quantities 10 μl for samples with concentration 30 ng/μl, 20 μl for 60 ng/μl and 40 μl for 120 ng/μl, correspondingly. The temperatures and thermocycler timings are specified in Figure 1d,e. After completion of the circularization step (Figure 1d), the Table 3 ingredients are added to the one-pot reaction tube for 30 ng/μl and 60 ng/μl input dsDNA concentrations, proceeding per Figure 1e, followed by spin-column cleanup Figure 1f using QIAquick PCR Purification Kit (QIAGEN 28106).

Table 3 Digestion reaction ingredients to add to each 100 μl of circularization reaction after heat inactivation for digestion step (Figure 1e)

Component	Per 100 μl reaction	Final conc.
30 ng/μl input DNA		
KOAc 1M (Thermo Fisher AAJ62817AE, pH 7.5)	6.5 μl	60 mM
T5 Exonuclease (NEB M0663, 10 units/μl)	2 μl	0.2 units/μl
60 ng/μl input DNA		
KOAc 1M (Thermo Fisher AAJ62817AE, pH 7.5)	6.6 μl	60 mM
T5 Exonuclease (NEB M0663, 10 units/μl)	4 μl	0.4 units/μl
120 ng/μl input DNA		
KOAc 1M (Thermo Fisher AAJ62817AE, pH 7.5)	12.0 μl	60 mM
T5 Exonuclease (NEB M0663, 10 units/μl)	8 μl	0.4 units/μl
Tris 1M (Invitrogen 15567027, pH 7.5)	2.5 μl	25 mM
$MgCl_2$ 1M (Technova M0303)	1.0 μl	10 mM
Nuclease-free H_2O (Invitrogen 10977015)	up to 100 μl	n/a

If the buffer is prepared for larger volumes or multiple digestion reactions, these ingredients may be scaled and combined, and added in specified combined volume to circularization reaction. For reactions with input DNA concentrations of 120 ng/μl, the reaction mixture is added in equal quantity to the ligation reaction buffer, thus KOAc and T5 exonuclease are calculated for 2X volume, while Tris and $MgCl_2$ compensate for the dilution of these components in the ligation reaction.

As a part of finetuning, we found that with the intended lower T5 exonuclease activity, digestion of reactions containing 120 ng/μl input dsDNA was not complete within one hour, likely owing to the high concentration of short linear fragments – byproduct of digestion, though full digestion was still achieved if digestion time was extended. To address this, we doubled the effective reaction volume for these samples by adding an equal amount of the digestion mix formulated in the third section of Table 3. This adjustment fully resolved the issue, achieving complete digestion within the intended one-hour timeframe.

These buffer optimizations successfully mitigated the risk of over-digestion highlighted above. Compared to the original method [9], the refined digestion step improved recovered yields for the shortest minicircles at high input DNA, while yields for longer minicircles remained essentially unchanged (see Supplementary Data for detailed comparisons), confirming that the moderated exonuclease activity and enhanced DNA stability effectively protected shorter minicircle products from gradual degradation. Another indication of the well-adjusted digestion method is virtually no DNA loss for the shortest minicircles at the lowest concentration; the gel image showed virtually complete circularization with minimal shadow of higher-order concatemers (Figure 2a, lane 0 min), matching the spin-column-recovered yield after digestion step and accounting for the experimentally determined column recovery rate. Taken together, these results validate the buffer adjustments as both protective against over-digestion of circular products and permissive for complete elimination of linear species.

The Excel spreadsheets for calculating and scaling reaction ingredients are available in the Supplementary Data.

Theoretical: Jacobson–Stockmayer estimates of DNA circularization efficiencies

Circularization efficiencies for linear double-stranded DNA fragments of 452, 552, 752, and 952 bp were estimated theoretically using the worm-like chain (WLC) model [4] and Jacobson-Stockmayer (JS) theory [1].

The Jacobson-Stockmayer factor (J), defined as the effective local concentration of one DNA end in the vicinity of the other (in molar units) [1], was approximated in the Gaussian (long-chain) limit of the WLC model [4]. Per Yamakawa (2016) [7] equation 7.39, the J-factor for longer dsDNA lengths L can be approximated by

$$J \propto L^{-3/2} \tag{1}$$

with L the DNA contour length (proportional to base-pair number). This power-law scaling arises from the probability density of end-to-end closure in three-dimensional random-walk chains in the large-N limit [1, 7].

The numerical computations are based on ring-closure probabilities in the twisted WLC model applied specifically to dsDNA parameters (persistence length $P \approx 50$ nm or $\sim$147 bp, helical repeat $\sim$10.5 bp/turn) [4]. The Shimada–Yamakawa calculations [4] show a broad peak in the effective concentration (directly related to the J-factor) in the range of tens of nM for contour lengths corresponding to $\sim$400–600 bp (for illustration see Fig. 5 in Shore et al. [3]), with the Gaussian $L^{-3/2}$ approximation providing a good fit in this regime and beyond for lengths $\gg 2P$.

From our experimental results, circularization efficiency is highest for the 452 bp fragment compared to longer fragments. In Supplementary Note 1 we evaluated the J-factor for this fragment lengths equal 86.0 nM (calibrated from the empirical cyclization efficiency of pre-cut overhangs at 120 ng/μl). Thus,

for calibration, J-factors were normalized such that the maximum value is 86 nM for the shortest fragment ($L_0 = 452$ bp).

For fragments of different lengths L_n, the relative scaling factor is $x = L_0/L_n$ and the J-factor is Equation 2:

$$J_n = J_0\, x^{-3/2} = 86.0 \times \left(\frac{L_n}{452}\right)^{-3/2} \tag{2}$$

(in nM); calculated J-factors (in nM) used here are presented in Table 4.

Table 4 Calculated J-factors per DNA length

DNA Length (bp)	J-factor (nM)
452	86.0
552	63.7
752	40.1
952	28.1

DNA mass concentrations (ng/μL) for each fragment length and experimental condition are presented in Table 5.

Table 5 DNA mass concentrations (ng/μL) and molar concentrations C for each fragment length

	DNA concentration		
DNA lengths (bp)	**Low**	**Medium**	**High**
Mass concentration of circularizable DNA (ng/μl)			
452	26.4	52.8	105.5
552	27.0	53.9	107.9
752	27.7	54.4	110.9
952	28.2	56.3	112.7
Molar concentration of circularizable DNA (nM)			
452	88.5	177.0	353.6
552	74.1	147.9	296.2
752	55.8	109.6	223.4
952	44.9	89.6	179.4

The input DNA concentrations are 30, 60 and 120 ng/μl, however as the input DNA is 62 bps longer to account for restriction enzyme sites and PCR adapters, which are cut off during the ligation/overhang cutting step. The resulting concentrations are smaller and slightly vary for each condition, thus for clarity here and later we call them low, medium and high concentrations. Corresponding molar concentrations C (nM), calculated using an average dsDNA molar mass of 660 g/mol per base pair.

The percentage efficiency for formation of monomeric circles was calculated from the kinetic competition between intramolecular cyclization (first-order rate proportional to J) and intermolecular dimerization (second-order rate

proportional to molar concentration C), yielding the circular monomer fraction [1, 13]:

$$\text{Monomer efficiency (\%)} = \frac{J}{J + 2C} \times 100 \tag{3}$$

The factor of 2 accounts for the stoichiometry of dimer formation consuming two molecules per ligation event.

For circular concatemers formed from x identical fragments ($x \geq 2$, integer; contour length xL_n), the J-factor scales as

$$J_x = \frac{J_1}{x^{3/2}} \tag{4}$$

according to the Gaussian-regime prediction of JS theory [1], similarly applied in Equation 1. Yields of circular concatemers (dimers, trimers, and higher-order species up to 16-mers) were estimated sequentially using the same kinetic branching model.

See resulting theoretical efficiencies for a circular monomer in Table 6 and total circularization efficiency combining monomers and all circular 2–16-mers in Table 7 (see the *Efficiency from J-Factor* sheet in the Supplementary Data spreadsheet *Circularization Efficiency.xlsx*).

Table 6 Monomeric circularization efficiency.

	DNA concentration		
DNA lengths (bp)	**Low (%)**	**Medium (%)**	**High (%)**
452	32.7	19.5	10.8
552	30.1	17.7	9.7
752	26.4	15.5	8.2
952	23.8	13.6	7.3

Calculations for fraction of circular dimers and trimers are presented in Supplementary Tables 1, 2.

Table 7 Total circularization efficiency as a sum of monomers and all circular 2–16-mers, used for comparison with experimental results in Table 1.

	DNA concentration		
DNA lengths (bp)	**Low (%)**	**Medium (%)**	**High (%)**
452	59.8	38.1	21.9
552	55.7	34.8	19.7
752	49.9	30.7	16.8
952	45.6	27.1	14.9

These values represent approximate theoretical yields for the specified circular species in an irreversible ligation reaction; the remainder consists of

linear oligomers (which are subsequently eliminated by T5 exonuclease digestion and spin-column purification steps). All percentages reflect the proportion of original DNA mass (or equivalently, incorporated original segments) in each circular form. Total circular efficiency (Table 7) is the sum of monomeric circles and all circular concatemers (higher-order species beyond 16-mers contribute negligibly).

Data availability

The unmodified gel image photos, the circularization efficiency spreadsheet and reaction reagents scaling spreadsheet are available in the Supplementary.PDF and SupplementaryData.ZIP file. The DNA sequences are available in the original publication [11].

Statistics and reproducibility

All protocol reactions were performed in independent reaction duplicates (n=2) as stated in figures, and yield percentage values were averaged.

Acknowledgments

The authors express their sincere gratitude to Davide Michieletto (School of Physics and Astronomy, and MRC Human Genetics Unit, University of Edinburgh) for his thoughtful discussions and expert insights with the Jacobson–Stockmayer model calculations.

Competing interests

GMC disclosures: https://arep.med.harvard.edu/gmc/tech.html

References

[1] Jacobson, H. & Stockmayer, W. H. Intramolecular reaction in polycondensations. I. The theory of linear systems. *The Journal of chemical physics* **18** (12), 1600–1606 (1950). https://doi.org/10.1063/1.1747547 .

[2] Dugaiczyk, A., Boyer, H. W. & Goodman, H. M. Ligation of EcoRI endonuclease-generated DNA fragments into linear and circular structures. *Journal of Molecular Biology* **96** (1), 171–184 (1975). https://doi.org/https://doi.org/10.1016/0022-2836(75)90189-8 .

[3] Shore, D., Langowski, J. & Baldwin, R. L. DNA flexibility studied by covalent closure of short fragments into circles. *Proceedings of the National Academy of Sciences* **78** (8), 4833–4837 (1981). https://doi.org/10.1073/pnas.78.8.483 .

[4] Shimada, J. & Yamakawa, H. Ring-closure probabilities for twisted wormlike chains. Application to DNA. *Macromolecules* **17** (4), 689–698 (1984). https://doi.org/10.1021/ma00134a028 .

[5] Taylor, W. H. & Hagerman, P. J. Application of the method of phage T4 DNA ligase-catalyzed ring-closure to the study of DNA structure: II. NaCl-dependence of DNA flexibility and helical repeat. *Journal of Molecular Biology* **212** (2), 363–376 (1990). https://doi.org/10.1016/0022-2836(90)90131-5 .

[6] Geggier, S. & Vologodskii, A. Sequence dependence of DNA bending rigidity. *Proceedings of the National Academy of Sciences* **107** (35), 15421–15426 (2010). https://doi.org/10.1073/pnas.1004809107 .

[7] Yamakawa, H. Chapter 7. Applications to Circular DNA. *Helical wormlike chains in polymer solutions* **1** (2016). https://doi.org/10.1007/978-3-662-48716-7 .

[8] Kricheldorf, H. R., Weidner, S. M. & Scheliga, F. Synthesis of cyclic polymers and flaws of the Jacobson–Stockmayer theory. *Polymer Chemistry* **11** (14), 2595–2604 (2020). https://doi.org/10.1039/D0PY00226G .

[9] Oliynyk, R. T. & Church, G. M. Efficient modification and preparation of circular DNA for expression in cell culture. *Communications Biology* **5** (1), 1393 (2022). https://doi.org/10.1038/s42003-022-04363-z .

[10] Bath, A. J., Milsom, S. E., Gormley, N. A. & Halford, S. E. Many type IIs restriction endonucleases interact with two recognition sites before cleaving DNA. *Journal of Biological Chemistry* **277** (6), 4024–4033 (2002). https://doi.org/10.1074/jbc.M108441200 .

[11] Oliynyk, R. T. & Church, G. M. Circular Vectors as an efficient, fully synthetic, cell-free approach for preparing small circular dna as plasmid substitute for guide RNA expression in CRISPR–Cas9 genome editing. *Nature Protocols* (2025). https://doi.org/10.1038/s41596-024-01138-0 .

[12] Trizna, L., Olajos, J. & Viglasky, V. DNA minicircles capable of forming a variety of non-canonical structural motifs. *Frontiers in Chemistry* **Volume 12 - 2024** (2024). https://doi.org/10.3389/fchem.2024.1384201 .

[13] Crothers, D. M., Drak, J., Kahn, J. D. & Levene, S. D. [1] DNA bending, flexibility, and helical repeat by cyclization kinetics. *Methods in enzymology* **212**, 3–29 (1992). https://doi.org/10.1016/0076-6879(92)12003-9 .